ADVANCED MATERIALS

[16] B. Skinner, *Am. Mineral.* **1960**, *45*, 612.
[17] A. K. Verma, T. B. Rauchfuss, S. R. Wilson, *Inorg. Chem.* **1995**, *34*, 3072.
[18] T. Sasaki, M. Watanabe, *J. Phys. Chem.* **1997**, *101*, 10 159.
[19] N. Pinna, K. Weiss, J. Urban, M.-P. Pileni, *Adv. Mater.* **2001**, *13*, 261.
[20] a) M. E. Spahr, P. Bitterli, R. Nesper, M. Müller, F. Krumeich, H.-U. Nissen, *Angew. Chem. Int. Ed.* **1998**, *37*, 1263. b) F. Krumeich, H.-J. Muhr, M. Niederberger, F. Bieri, B. Schnyder, R. Nesper, *J. Am. Chem. Soc.* **1999**, *121*, 8324. c) H.-J. Muhr, F. Krumeich, U. P. Schönholzer, F. Bieri, M. Niederberger, L. J. Gauckler, R. Nesper, *Adv. Mater.* **2000**, *12*, 231. d) M. Niederberger, H.-J. Muhr, F. Krumeich, F. Bieri, D. Günther, R. Nesper, *Chem. Mater.* **2000**, *12*, 1995.
[21] P. Hirsch, A. Howie, R. B. Nicholson, D. W. Pashley, M. J. Whelan, in *Electron Microscopy of Thin Crystals* (Ed: R. E. Krieger), Huntington, New York **1977**, Ch. 5, p. 117.
[22] a) M. Shinada, S. Sugano, *J. Phys. Soc. Jpn.* **1966**, *21*, 1936. b) C. J. Sandroff, D. M. Hwang, W. M. Chung, *Phys. Rev. B* **1986**, *33*, 5953. c) C. J. Sandroff, S. P. Kelty, D. M. Hwang, *J. Chem. Phys.* **1986**, *85*, 2237.
[23] Y. Wang, N. Herron, *J. Phys. Chem.* **1991**, *95*, 5054.
[24] In order to evaluate the average thickness of the nanosheets, the bandgap energy shift, $\Delta E_g$, by exciton confinement in anisotropic two-dimensional crystallites is formulated as [22]:

$$\Delta E_g \approx \frac{h^2}{8\mu_{xz}}\left(\frac{1}{L_x^2}+\frac{1}{L_z^2}\right)+\frac{h^2}{8\mu_y L_y^2} \quad (1)$$

where $h$ is Planck's constant, $\mu_{xz}$, $\mu_y$ are the reduced effective mass of the exciton, and $L_x$, $L_y$, $L_z$ are crystallite dimensions. Since $L_x, L_z \gg L_y$ for the nanosheet, the first term can be ignored, therefore the blue shift is predominantly governed by the sheet thickness:

$$\Delta E_g \approx \frac{h^2}{8\mu_y L_y^2} \quad (2)$$

The bandgap of ZnS nanosheets can be estimated by fitting the absorption data to the direct transition equation [23]:

$$\alpha \times h\nu = A\,(h\nu - E_g)^{1/2} \quad (3)$$

where $\alpha$ is the absorption coefficient, $h\nu$ is the photo-energy, $E_g$ is the direct bandgap, and $A$ is a constant. In the case of the ZnS nanosheet, the parameters for calculation are: $E_{g(bulk)} = 3.80$ eV, $E_g = 5.08$ eV, $m_{e^-} = 0.42$, $m_{h^+} = 0.61$, $\Delta E_g = 1.16$ eV, $\mu_y = 0.2487$. The calculated thickness of ZnS nanosheets is about 11 Å. The nanosheet thickness is much smaller than the exciton Bohr radius $a_B = 22$ Å for wurtzite ZnS.
[25] S. A. Empedocles, R. Neuhauser, K. Shimizu, M. G. Bawendi, *Adv. Mater.* **1999**, *15*, 1243.

## Biomimetic Morphogenesis of Calcium Carbonate in Mixed Solutions of Surfactants and Double-Hydrophilic Block Copolymers**

By *Limin Qi*,* *Jie Li*, and *Jiming Ma*

The chemical synthesis of inorganic materials with unusual and complex forms, a chemistry of form,[1] has attracted considerable attention owing to the obvious importance of the shape and texture of materials in determining their properties. It is well-known that biominerals are distinguished by a complexity of form well-suited to their functions. The strategy of using organic templates and/or additives to control the nucleation, growth, and alignment of inorganic particles has been widely applied to the biomimetic morphogenesis of inorganic materials with complex forms.[1–6]

The biomimetic synthesis of calcium carbonate ($CaCO_3$), one of the most abundant biominerals, has been intensively investigated. Langmuir monolayers,[7] self-assembled monolayers (SAMs),[8] crystal-imprinted polymer surfaces,[9] and crosslinked gelatin films[10] have been used as templates or matrices for the controlled growth of $CaCO_3$ crystals. Interestingly, SAM-coated gold colloids were used as curved templates, or nuclei, for the crystallization of calcite spherules.[11] On the other hand, a variety of macromolecular additives, including biomacromolecules,[12] a designed peptide,[13] and dendrimers,[14] have exhibited large influences on $CaCO_3$ crystallization. Notably, the biomimetic synthesis of $CaCO_3$ thin films has been achieved by using the cooperative effect of organic substrates and soluble polymeric additives.[15] Moreover, structured three-dimensional media, such as emulsion foams,[16] water-in-oil microemulsions,[17] and a pseudovesicular double emulsion,[18] have been used as templates for the ingenious morphogenesis of $CaCO_3$ (vaterite or aragonite) hollow spheres with various surface patterns.

Recently, double-hydrophilic block copolymers (DHBC)[19] have been used as a new class of additives for the effective control of the morphology of inorganic crystals such as $BaSO_4$,[6] calcium phosphate,[20] and $CaCO_3$.[21,22] Considering that the strong interaction between polymers and surfactants can result in polymer–surfactant complexes that form complex structures in aqueous solution,[23] it is expected that the morphogenesis of inorganic minerals with unusual morphologies can be achieved by using aqueous DHBC–surfactant mixtures. In this communication, we report on the first synthesis of $CaCO_3$ (calcite) hollow spheres by the cooperative effect of DHBC–surfactant complex micelles as templates and free DHBC molecules as inhibitors. In addition, uniform vaterite discs and unusual calcite pine-cone shaped particles have been facilely produced in mixed DHBC–surfactant systems.

In this work, we studied the mixed poly(ethylene oxide)-*block*-poly(methacrylic acid)–sodium dodecylsulfate (PEO-*b*-PMAA–SDS) system; the crystallization of $CaCO_3$ was conducted at room temperature, according to the literature procedure.[21a] At an SDS concentration lower than 0.1 mM, only calcite spheres or dumb-bell like particles were produced, essentially the same as has been observed in the single PEO-*b*-PMAA system.[21a] However, when the SDS concentration was increased to 1 or 2 mM, well-defined $CaCO_3$ hollow spheres were obtained. The related X-ray diffraction (XRD) pattern exhibited sharp reflections at 0.386, 0.303, 0.250, 0.228, 0.210, 0.191, and 0.187 nm, consistent with the (102), (104), (110), (113), (202), (108), and (116) reflections of calcite. This suggests that the hollow spheres consist of calcite, the most stable polymorph of $CaCO_3$. Figure 1 presents typical scanning electron microscopy (SEM) images of the calcite hollow spheres obtained at an SDS concentration of 2 mM. The SEM image shown in Figure 1a suggests that the sizes of the calcite hollow spheres range from 2.5 to 4 μm, with an average size of ca. 3.4 μm. A few partly broken hollow

[*] Prof. L. Qi, J. Li, Prof. J. Ma
College of Chemistry, Peking University
Beijing 100 871 (China)
E-mail: liminqi@chem.pku.edu.cn

[**] This work was supported by NSFC (20 003 001, 29 733 110), the Special Fund of MEC (No. 200 020), and the Doctoral Program Foundation of MEC.

  0935-9648/02/0402-0300 $ 17.50+.50/0 

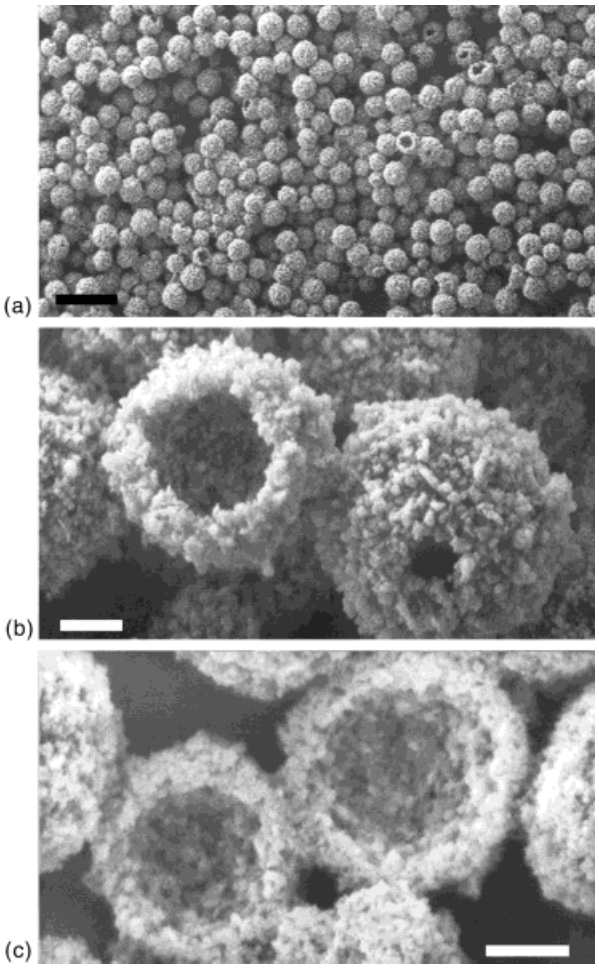


Fig. 1. a) SEM image of calcite hollow spheres formed in mixed PEO-*b*-PMAA–SDS solutions before sonication. b) High-magnification SEM image of two broken calcite hollow spheres. c) High-magnification SEM image of calcite hollow spheres after sonication. [SDS] = 2 mM. Scale bars: a) 10 μm, b) 1 μm, c) 1 μm.

spheres were clearly observed, but there was less than 3 % of these. Figure 1b shows a high-magnification SEM image of two broken hollow spheres, which exhibited rough outer surfaces apparently consisting of primary particles ranging from tens to hundreds of nanometers in size.

Interestingly, the hollow spheres can be broken by simple sonication. For example, nearly 40 % of the hollow spheres were broken after they were sonicated for 2 min before the SEM sample preparation. A high-magnification SEM image of these broken hollow spheres (Fig. 1c) shows the rough inner surfaces of the hollow shells, similar to their outer surfaces, further indicating the polycrystalline nature of the walls. From this image, the wall thickness was estimated to be about 0.5 μm. However, it is still difficult to discern whether the primary calcite crystals were misoriented or radially oriented with their *c* axes parallel to the sphere surface. Further investigation into this may provide information that will add to our understanding of the nucleation mechanism. To the best of our knowledge, this is the first report of the synthesis of micrometer-sized calcite hollow spheres. Since calcite is more stable than the other two polymorphs of $CaCO_3$, i.e., aragonite and vaterite, it is possible that calcite hollow spheres will be useful in more applications than aragonite[16] and vaterite[17,18,21b] hollow spheres.

Increasing the SDS concentration in the mixed PEO-*b*-PMAA–SDS solution further, to 5 or 10 mM, resulted in the formation of uniform vaterite discs instead of calcite hollow spheres. A typical SEM image of the unique crystals obtained at an SDS concentration of 10 mM is presented in Figure 2a, and this suggests that the crystals are uniform convex discs with an average size of 1.4 μm, reminiscent of the single crystal vaterite discs prepared under stearic acid monolayers.[24] However, the present discs were much thinner, with a thickness of less than 0.2 μm, resulting in a much larger aspect ratio. Figure 2b presents a TEM image of a single disc, and the related electron diffraction (ED) pattern. The ED pattern was obtained from an area including the whole disc, since the disc was thin enough for the electron beam. According to the indexation of the ED pattern, the disc is a vaterite single crystal lying on the (001) plane, similar to the vaterite discs mentioned above. This result is consistent with the corresponding XRD result, which shows considerably intensified (002) and

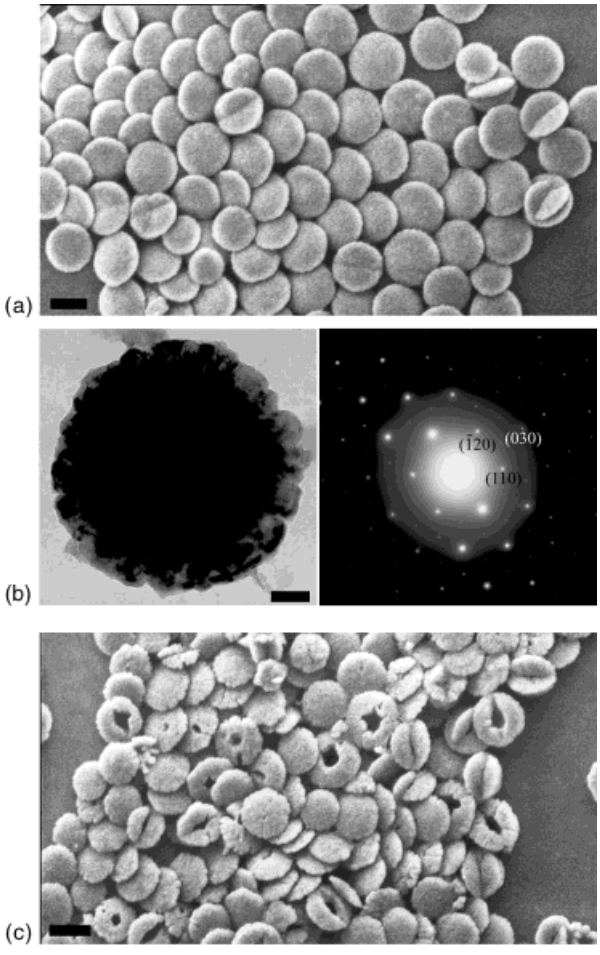


Fig. 2. SEM images of the vaterite discs formed in mixed PEO-*b*-PMAA–SDS solutions after 1 day (a,b) and 7 days (c) of aging. The ED pattern of the disc shown in (b) is presented on the right side of (b), which corresponds to the [001] zone of vaterite. [SDS] = 10 mM. Scale bars: a) 1 μm, b) 0.2 μm, c) 1 μm.

  0935-9648/02/0402-0301 $ 17.50+.50/0 

ADVANCED MATERIALS

(004) vaterite reflections (compared to their typical intensities), which suggests that the (001) plane was preferentially aligned along the specimen surface due to the preferential spreading of the vaterite discs parallel to the specimen surface. Another interesting finding is that hollow discs were formed when the vaterite discs were aged in their mother solution for a longer time (e.g., 1 week). Obviously, the hollow discs were formed by partial dissolution of the central regions of the discs (Fig. 2c), in a manner basically similar to that reported for the formation of torus-shaped vaterite particles in SDS solution after 1 day of dissolution.[17] However, the present hollow discs were much smaller, and the dissolution of their central part seemed much slower, indicating the role of the polymer in preventing the vaterite discs from dissolving.

For comparison, we also investigated the $CaCO_3$ crystallization in mixed solutions of PEO-*b*-PMAA and cetyltrimethylammonium bromide (CTAB), a typical cationic surfactant. In this system, according to the XRD measurements, only calcite crystals were produced. It was observed that only calcite spheres and dumb-bells, as in the single PEO-*b*-PMAA system, were obtained when the CTAB concentration was lower than 0.1 mM. Increasing the concentration of CTAB to 0.5 mM resulted in only peanut-shaped crystals being produced. Strikingly, uniform pine-cone shaped calcite crystals (~3 μm in length and 1.2 μm in diameter) were formed when the CTAB concentration was increased to 1 mM (Fig. 3a). The detailed morphology of a single pine-cone is illustrated in a high-magnification SEM image (Fig. 3b), which roughly shows the appearance of newly developed crystal faces other than the rhombohedral calcite {104} surfaces. If the CTAB concentration was further increased to 2 mM or higher, *c*-axis elongated calcite crystals exhibiting obvious {104} caps and macrosteps were obtained (Fig. 3c). These results indicate that with increasing CTAB concentration, the calcite crystals gradually recovered their rhombohedral {104} faces, probably due to the impairment of the inhibition efficiency of the polymer on the non-rhombohedral surfaces caused by the electrostatic interaction between the CTAB and PMAA segments.

We turn now to the consideration of the formation mechanism of the calcite hollow spheres in the mixed PEO-*b*-PMAA–SDS system. It has been reported that the PEO-*b*-PMAA type DHBC can form DHBC–surfactant complexes with a variety of cationic surfactants.[19] In aqueous solution, the PEO-*b*-PMAA–cationic surfactant complexes can form micelle-like aggregates with a core of polyanion segments neutralized by surfactant cations, and a shell of PEO segments.[23b] Since the polyanionic PMAA block is the strongly interacting block for $CaCO_3$, it is expected that the core–shell micelles formed by the PEO-*b*-PMAA–CTAB complex with a PEO corona would not play the role of template for the $CaCO_3$ crystallization. On the other hand, it is well known that the homopolymer PEO can interact strongly with anionic SDS to form PEO-SDS complex micelles with EO groups intermingling in the head group region of the SDS micelles.[23a] Therefore, it is reasonable to assume that core–shell micelles can be formed by a PEO-*b*-PMAA–SDS complex with a core

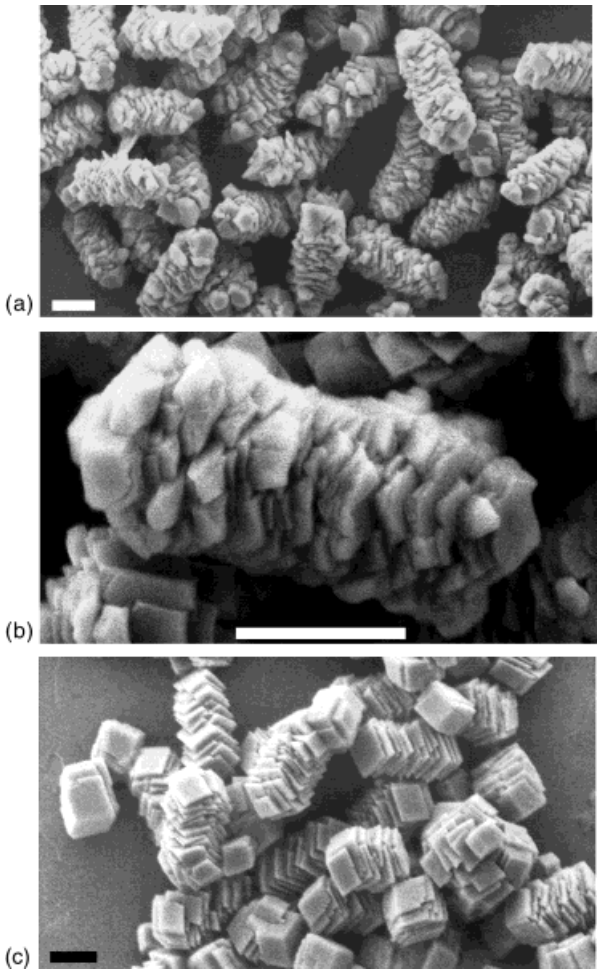


Fig. 3. SEM images of the calcite crystals formed in mixed PEO-*b*-PMAA–CTAB solutions. a,b) [CTAB] = 1 mM. c) [CTAB] = 2 mM. Scale bars = 1 μm.

of PEO segments solubilized in the head group region of the SDS micelles, and a shell of PMAA segments. Such core–shell micelles, with a PMAA corona, would act as templates for the $CaCO_3$ crystallization. Meanwhile, the free PEO-*b*-PMAA molecules in solution act as potent inhibitors. The cooperative effect of the templates and the inhibitors would finally lead to the formation of calcite hollow spheres around the PEO-*b*-PMAA–SDS complex micelles. If the SDS concentration is too large, probably only bound PEO-*b*-PMAA molecules are present, along with many pure SDS micelles, leading to the formation of vaterite discs.

This interpretation indicates that the presence of both PMAA and PEO segments is necessary for the formation of core–shell micelles, and thus calcite hollow spheres. This is consistent with the observation that only calcite solid spheres were produced in mixed PMAA–SDS solutions, whereas rhombohedral calcite crystals were formed in mixed PEO-SDS solutions under similar conditions. Furthermore, our dynamic light scattering (DLS) measurements revealed the presence of large aggregates in the original polymer solutions. The scattering intensity of a pure PEO-*b*-PMAA solution (1 g $L^{-1}$, pH 10) was very weak, excluding the presence of any aggregates larger

  0935-9648/02/0402-0302 $ 17.50+.50/0 

than 10 nm. When SDS (2 mM) was present in this solution, the scattering intensity was increased significantly, and an average aggregate size of 165 nm was obtained from the DLS measurement, indicating the formation of PEO-*b*-PMAA–SDS complex micelles. If $CaCl_2$ (0.4 mM) was also present in the mixed PEO-*b*-PMAA–SDS solution, the average size of the aggregates increased to 180 nm, suggesting that the presence of salts has a considerable effect on the size of the complex micelles. It is noteworthy that the aggregate size seems much smaller than the inner diameter of the calcite hollow spheres obtained (larger than 1 μm); however, the proposed mechanism is still reasonable, considering that both the presence of the reactants in the solution and the development of the inorganic structure could perturb the organic template, resulting in an adaptive construction.[1] Moreover, there could be a microscopic phase separation of polymer–surfactant droplets that is further stabilized by the adsorption of calcite primary crystallites around the external surface of individual drops. A detailed time course study was expected to provide direct evidence for such a speculation; unfortunately, our preliminary experiments showed that there was an outburst of $CaCO_3$ precipitation in the solution after a short induction period and hence the hollow spheres were formed very quickly, which prevented the direct observation of their detailed formation process.

In conclusion, calcite hollow spheres have been successfully synthesized, for the first time, by the cooperative effect of DHBC–surfactant complex micelles as templates and free DHBC molecules as inhibitors. Moreover, unique vaterite discs and unusual calcite pine-cone shaped particles have also been facilely produced in the mixed DHBC–surfactant systems. The superstructures of the new minerals obtained here may make them promising candidates for materials science due to the importance of shape and texture in determining the properties of materials. The formation of calcite hollow spheres in mixed DHBC–surfactant solutions represents a novel method of preparing inorganic hollow spheres—a topic of intense interest.[25]

## *Experimental*

A commercial DHBC, poly(ethylene oxide)-*block*-poly (methacrylic acid) (PEO-*b*-PMAA, PEO = 3000 g/mol, PMAA = 700 g/mol, Th. Goldschmidt AG) [21], was used in this work. The anionic PMAA block carries carboxylate groups capable of coordinating with $Ca^{2+}$ ions, whereas the nonionic PEO block mainly promotes solubilization in water. The crystallization of $CaCO_3$ was conducted at room temperature (ca. 22 °C) following the reported procedure [21a], except for the addition of either the anionic surfactant sodium dodecylsulfate (SDS) or the cationic surfactant cetyltrimethylammonium bromide (CTAB). Typically, a solution of $Na_2CO_3$ (0.5 M, 0.32 mL) was injected into 20 mL of a mixed solution of PEO-*b*-PMAA (1 $g\,L^{-1}$) and SDS or CTAB (varied concentrations, e.g., 2 mM). After the pH of the solution was adjusted to 10, a solution of $CaCl_2$ (0.5 M, 0.32 mL) was added under vigorous stirring. After 1 min of stirring, the solution was allowed to stand for 24 h before the product was collected and characterized with scanning electron microscopy (SEM), transmission electron microscopy (TEM) and X-ray diffraction (XRD).

*Dynamic Light Scattering*: DLS measurements were performed on a laboratory-built goniometer with a Langley-Ford 1069 digital correlator and a Spectra-Physics argon ion laser, at a wavelength of 514.5 nm.

Received: September 10, 2001
Final version: November 13, 2001

[1] S. Mann, *Angew.Chem. Int. Ed.* **2000**, *39*, 3392.
[2] S. Mann, G. A. Ozin, *Nature* **1996**, *382*, 313.
[3] R. Kniep, S. Busch, *Angew. Chem. Int. Ed. Engl.* **1996**, *35*, 2624.
[4] H. Yang, N. Coombs, G. A. Ozin, *Nature* **1997**, *386*, 692.
[5] M. Antonietti, F Gröhn, J. Hartmann, L. Bronstein, *Angew. Chem. Int. Ed. Engl.* **1997**, *39*, 2080.
[6] L. Qi, H. Cölfen, M. Antonietti, *Angew. Chem. Int. Ed.* **2000**, *39*, 604.
[7] a) A. L. Litvin, S. Valiyaveettil, D. L. Kaplan, S. Mann, *Adv. Mater.* **1997**, *9*, 124. b) J. Lahiri, G. Xu, D. M. Dabbs, N. Yao, I. A. Aksay, J. T. Groves, *J. Am. Chem. Soc.* **1997**, *119*, 5449. c) S. Champ, J. A. Dickinson, P. S. Fallon, B. R. Heywood, M. Mascal, *Angew. Chem. Int. Ed.* **2000**, *39*, 2716.
[8] a) J. Aizenberg, A. J. Black, G. M. Whitesides, *Nature* **1999**, *398*, 495. b) J. Küther, G. Nelles, R. Seshadri, M. Schaub, H.-J. Butt, W. Tremel, *Chem. Eur. J.* **1998**, *4*, 1834.
[9] S. M. D'Souza, C. Alexander, S. W. Carr, A. M. Waller, M. J. Whitcombe, E. N. Vulfson, *Nature* **1999**, *398*, 312.
[10] a) G. Falini, S. Fermani, M. Gazzano, A. Ripamonti, *Chem. Eur. J.* **1997**, *3*, 1807. b) G. Falini, S. Fermani, M. Gazzano, A. Ripamonti, *Chem. Eur. J.* **1998**, *4*, 1048.
[11] J. Küther, R. Seshadri, W. Tremel, *Angew. Chem. Int. Ed.* **1998**, *37*, 3044.
[12] a) A. M. Belcher, X. H. Wu, R. J. Christensen, P. K. Hansma, G. D. Stucky, D. E. Morse, *Nature* **1996**, *381*, 56. b) G. Falini, S. Albeck, S. Weiner, L. Addadi, *Science* **1996**, *271*, 67.
[13] D. B. DeOliveira, R. A. Laursen, *J. Am. Chem. Soc.* **1997**, *119*, 10 627.
[14] a) K. Naka, Y. Tanaka, Y. Chujo, Y. Ito, *Chem. Commun.* **1999**, 1931. b) J. Donners, B. R. Heywood, E. Meijer, R. Nolte, C. Roman, A. Schenning, N. Sommerdijk, *Chem. Commun.* **2000**, 1937.
[15] a) G. Xu, N. Yao, I. A. Aksay, J. T. Groves, *J. Am. Chem. Soc.* **1998**, *120*, 11 977. b) A. Sugawara, T. Kato, *Chem. Commun.* **2000**, 487.
[16] D. Walsh, S. Mann, *Nature* **1995**, *377*, 320.
[17] D. Walsh, B. Lebeau, S. Mann, *Adv. Mater.* **1999**, *11*, 324.
[18] T. Hirai, S. Hariguchi, I. Komasawa, R. J. Davey, *Langmuir* **1997**, *13*, 6650.
[19] A recent review: H. Cölfen, *Macromol. Rapid Commun.* **2001**, *22*, 219.
[20] M. Antonietti, M. Breulmann, C. G. Göltner, H. Cölfen, K. K. Wong, D. Walsh, S. Mann, *Chem. Eur. J.* **1998**, *4*, 2493.
[21] a) H. Cölfen, L. Qi, *Chem. Eur. J.* **2001**, *7*, 106. b) H. Cölfen, M. Antonietti, *Langmuir* **1998**, *14*, 582.
[22] J. M. Marentette, J. Norwig, E. Tockelmann, W. H. Meyer, G. Wegner, *Adv. Mater.* **1997**, *9*, 647.
[23] a) G. Wang, G. Olofsson, *J. Phys. Chem. B* **1998**, *102*, 9276. b) T. K. Bronich, A. M. Popov, A. Eisenberg, V. A. Kabanov, A. V. Kakanov, *Langmuir* **2000**, *16*, 481.
[24] S. Mann, B. R. Heywood, S. Rajam, J. D. Birchall, *Nature* **1988**, *334*, 692.
[25] a) F. Caruso, *Chem. Eur. J.* **2000**, *6*, 413. b) Z. Zhong, Y. Yin, B. Gates, Y. Xia, *Adv. Mater.* **2000**, *12*, 206. c) B. Putlitz, K. Landfester, H. Fischer, M. Antonietti, *Adv. Mater.* **2001**, *13*, 500.

## Regular Alumina Nanopillar Arrays**

By *Zhihao Yuan*, *Hua Huang*, and *Shoushan Fan**

Low-dimensional nanomaterials (i.e., nanodots, nanowires, nanotubes, nanopillars, and nanorods) have received considerable attention over the past decade because of their unique properties as well as their potentially wide applications in magnetic, electronic, and optoelectronic structures and devices.[1–6] For the preparation of the low-dimensional nano-

[*] Prof. S. S. Fan, Z. H. Yuan,[+] H. Huang
Department of Physics, Tsinghua University
Beijing 100084 (China)
E-mail: fss-dmp@mail.tsinghua.edu.cn
[+] Second address: Department of Chemistry, Tsinghua University, Beijing 100084, China.

[**] The authors thank Prof. Y. D. Li, Prof. N. F. Gao, Dr. L. Liu, Dr. Y. J. Yan, and Dr. D. R. Ou for their cooperation and help. This work was supported by the National Natural Science Foundation of China and the State Key Project of Fundamental Research of China.

  0935-9648/02/0402-0303 $ 17.50+.50/0 